

# Template-Assisted Self-Assembly: A Practical Route to Complex Aggregates of Monodispersed Colloids with Well-Defined Sizes, Shapes, and Structures

Yadong Yin,<sup>§</sup> Yu Lu,<sup>§</sup> Byron Gates,<sup>†</sup> and Younan Xia<sup>†,\*</sup>

Contribution from the Departments of Chemistry and Materials Science & Engineering, University of Washington, Seattle, Washington 98195-1700

Received April 25, 2001

**Abstract:** This paper describes a strategy that combines physical templating and capillary forces to assemble monodispersed spherical colloids into uniform aggregates with well-controlled sizes, shapes, and structures. When an aqueous dispersion of colloidal particles was allowed to dewet from a solid surface that had been patterned with appropriate relief structures, the particles were trapped by the recessed regions and assembled into aggregates whose structures were determined by the geometric confinement provided by the templates. We have demonstrated the capability and feasibility of this approach by assembling polystyrene beads and silica colloids ( $\geq 150$  nm in diameter) into complex aggregates that include polygonal or polyhedral clusters, linear or zigzag chains, and circular rings. We have also been able to generate hybrid aggregates in the shape of HF or H<sub>2</sub>O molecules that are composed of polymer beads having different diameters, polymer beads labeled with different organic dyes, and a combination of polymeric and inorganic beads. These colloidal aggregates can serve as a useful model system to investigate the hydrodynamic and optical scattering properties of colloidal particles having nonspherical morphologies. They should also find use as the building blocks to generate hierarchically self-assembled systems that may exhibit interesting properties highly valuable to areas ranging from photonics to condensed matter physics.

## Introduction

Colloidal particles are small objects with at least one characteristic dimension in the range of 1 nm to 1  $\mu$ m. They have long been used as major components of various industrial products such as foods, drinks, inks, paints, toners, coatings, papers, cosmetics, photographic films, and rheological fluids.<sup>1</sup> They have also been extensively studied in the context of materials science, chemistry, biology, condensed matter physics, applied optics, or fluid dynamics.<sup>2</sup> The ability to synthesize colloidal particles that are uniform in size, shape, composition, and properties (both surface and bulk) has played an extremely important role in elucidating and understanding the optical, rheological, and electrokinetic behaviors of these materials.<sup>3</sup> Many advances in this area were mainly brought on by the elaboration of simple, convenient, and reproducible methods that were capable of generating monodispersed colloids in relatively precise quantities.

Spherical colloids have been the dominant subject of research for many decades due to their ease of production as monodis-

persed samples.<sup>3</sup> Driven by the minimization of interfacial energy, a sphere represents the simplest form that colloidal particles easily adopt during the nucleation or growth process. A wide variety of chemical methods have now been developed to generate spherical colloids from a range of different materials such as organic polymers and inorganic compounds.<sup>4</sup> It has also been possible to achieve a precise control over the properties of spherical colloids by changing their intrinsic parameters such as the diameter, chemical composition, bulk substructure, crystallinity (polycrystalline versus amorphous), and surface functional group (thus the surface charge density and interfacial free energy).<sup>5</sup> Studies on the spherical system have enriched our understanding on the interactions between colloidal particles, as well as their hydrodynamics in various types of dispersion media.<sup>6</sup> On the other hand, spherical colloids may also represent the simplest form of building blocks that could be readily self-assembled into three-dimensionally ordered lattices such as colloidal crystals or synthetic opals.<sup>7</sup> The ability to crystallize spherical colloids into spatially periodic structures has allowed us to obtain interesting and often useful functionality not only from the colloidal materials, but also from the long-range order

\* To whom correspondence should be addressed: (e-mail) xia@chem.washington.edu.

<sup>§</sup> Department of Materials Science & Engineering.

<sup>†</sup> Department of Chemistry.

(1) Books on colloidal science: (a) Russel, W. B.; Saville, D. A.; Schowalter, W. R. *Colloidal Dispersions*; Cambridge University Press: New York, 1989. (b) Everett, D. H. *Basic Principles of Colloid Science*; Royal Society of Chemistry: London, 1988. (c) Hunter, R. J. *Introduction to Modern Colloid Science*; Oxford University Press: Oxford, 1993.

(2) Recent reviews: (a) Murray, C. A.; Grier, D. G. *Am. Sci.* **1995**, *83*, 238. (b) Grier, D. G., Ed. From Dynamics to Devices: Directed Self-Assembly of Colloidal Materials, a special issue in: *MRS Bull.* **1998**, *23* (10), 21. (c) Gast, A. P.; Russel, W. B. *Phys. Today* **1998**, *December*, 24.

(3) Some recent reviews: (a) Xia, Y.; Gates, B.; Yin, Y.; Lu, Y. *Adv. Mater.* **2000**, *12*, 693. (b) Matijevic, E. *Langmuir* **1994**, *10*, 8. (c) Matijevic, E., Ed. Fine Particles, a special issue in: *MRS Bulletin*, **1989**, *14* (12), 18.

(4) See, for example: (a) Stöber, W.; Fink, A. *J. Colloid Interface Sci.* **1968**, *26*, 62. (b) Iler, R. K. *The Chemistry of Silica*; Wiley-Interscience: New York, 1979. (c) *Emulsion Polymerization*; Piirma, I., Ed.; Academic Press: New York, 1982. (d) *Science and Technology of Polymer Colloids*; Poehlein, G. W., Ottewill, R. H., Goodwin J. W., Eds.; Martinus Nijhoff Publishers: Boston, 1983; Vol. II.

(5) (a) Matijevic, E. *Acc. Chem. Res.* **1981**, *14*, 22. (b) Matijevic, E. *Chem. Mater.* **1993**, *5*, 412.

(6) See, for example: (a) Mie, G. *Ann. Phys.* **1908**, *25* (4), 377. (b) Larsen, A. E.; Grier, D. G. *Nature* **1997**, *385*, 230.

(7) (a) Dinsmore, A. D.; Crocker, J. C.; Yodel, A. G. *Curr. Opin. Colloid Interface* **1998**, *3*, 5. (b) Pieranski, P. *Contemp. Phys.* **1983**, *24*, 25. (c) van Megan, W.; Snook, I. *Adv. Colloid Interface Sci.* **1984**, *21*, 119.

exhibited by these crystalline lattices.<sup>8</sup> The beautiful, iridescent colors of an opal, for instance, are largely caused by the highly ordered lattice of silica colloids that are colorless by themselves.<sup>9</sup> Studies on the optical properties of these materials have now evolved into a new and active field of research that is often referred to as photonic crystals or photonic band gap (PBG) structures.<sup>10</sup>

Although spherical colloids will continue to play a predominant role in colloid science, they are not necessarily the best option for all fundamental studies or real-world applications that are associated with colloidal particles. They cannot, for example, exactly model the interactions between and hydrodynamic behaviors of highly irregular colloids that are more commonly found in industrial products.<sup>1</sup> They can only provide a very limited set of crystal structures when they are used as the building blocks to form periodic arrays. Theoretical studies have also indicated that they are not well-suited as the building blocks in generating photonic crystals with complete band gaps due to degeneracy in the photonic band structure caused by the spherical symmetry of the lattice points.<sup>11</sup> In this regard, nonspherical particles will offer some immediate advantages over their spherical counterparts in applications that require lattices with lower symmetries and higher complexities. Although a wealth of chemical methods have been developed for preparing spherical colloids (e.g., polymer latexes or silica beads) as monodispersed systems,<sup>4</sup> only a few approaches are available for producing nonspherical colloids as truly monodispersed samples, in which the shape, size, and charge chemically fixed on the surface are identical to within 2%.<sup>12–15</sup>

(8) See, for example: (a) Holtz, J. H.; Asher, S. A. *Nature* **1997**, *389*, 829. (b) Chang, S.-Y.; Liu, L.; Asher, S. A. *J. Am. Chem. Soc.* **1994**, *116*, 6739. (c) Weissman, J. M.; Sunkara, H. B.; Tse, A. S.; Asher, S. A. *Science* **1996**, *274*, 959. (d) Sunkara, H. B.; Jethmalani, J. M.; Ford, W. T. *Chem. Mater.* **1994**, *6*, 362.

(9) Sanders, J. V. *Nature* **1964**, *204*, 1151

(10) (a) Velev, O. D.; Jede, T. A.; Lobo, R. F.; Lenhoff, A. M. *Nature* **1997**, *389*, 447. (b) Holland, B. T.; Blanford, C. F.; Stein, A. *Science* **1998**, *281*, 538. (c) Park, S. H.; Xia, Y. *Chem. Mater.* **1998**, *10*, 1745. (d) Yang, P.; Deng, T.; Zhao, D.; Feng, P.; Pine, D.; Chmelka, B. F.; Whitesides, G. M.; Stucky, G. D. *Science* **1998**, *282*, 2244. (e) Wijnhoven, J. E. G. J.; Vos, W. L. *Science* **1998**, *281*, 802. (f) Zakhidov, A. A.; Baughman, R. H.; Iqbal, Z.; Cui, C.; Khayrullin, I.; Dantas, S. O.; Marti, J.; Ralchenko, V. G. *Science* **1998**, *282*, 897. (g) Johnson, S. A.; Ollivier, P. J.; Mallouk, T. E. *Science* **1999**, *283*, 963. (h) Vlasov, Y. A.; Yao, N.; Norris, D. J. *Adv. Mater.* **1999**, *11*, 165. (i) Subramanian, G.; Manoharan, V. N.; Thorne, J. D.; Pine, D. J. *Adv. Mater.* **1999**, *11*, 1261. (j) Jiang, P.; Cizeron, J.; Bertone, J. F.; Colvin, V. L. *J. Am. Chem. Soc.* **1999**, *121*, 7957. (k) Braun, P. V.; Wiltzius, P. *Nature* **1999**, *402*, 603. (l) Blanco, A.; Chomski, E.; Grabtchak, M. I.; John, S.; Leonard, S. W.; Lopez, C.; Meseguer, F.; Miguez, H.; Mondia, J. P.; Ozin, G. A.; Toader, O.; van Driel, H. M. *Nature* **2000**, *405*, 437. (m) Tarhan, I. I.; Watson, G. H. *Phys. Rev. Lett.* **1996**, *76*, 315. (n) Mayoral, R.; Requena, J.; Moya, J. S.; López, C.; Cintas, A.; Míguez, H.; Meseguer, F.; Vázquez, L.; Holgado, M.; Blanco, A. *Adv. Mater.* **1997**, *9*, 257.

(11) See, for example: (a) Li, Z. Y.; Wang, J.; Gu, B. Y. *J. Phys. Soc. Jpn.* **1998**, *67*, 3288. (b) Xia, Y.; Gates, B.; Li, Z.-Y. *Adv. Mater.* **2001**, *13*, 409.

(12) Ellipsoidal polymer beads formed by uniaxially stretching spherical beads: (a) Sutura, S. P.; Boylan, C. W. *J. Colloid Interface Sci.* **1980**, *73*, 29. (b) Nagy, M.; Keller, A. *Polym. Commun.* **1989**, *30*, 130. (c) Keville, K. M.; Franes, E. I.; Caruthers, J. M. *J. Colloid Interface Sci.* **1991**, *144*, 103. (d) Jiang, P.; Bertone, J. F.; Colvin, V. L. *Science* **2001**, *291*, 453. (e) Lu, Y.; Yin, Y.; Xia, Y. *Adv. Mater.* **2001**, *13*, 271.

(13) Ellipsoidal hematite particles formed using a gel-sol process: (a) Osaki, M.; Kratochvil, S.; Matjevic, E. *J. Colloid Interface Sci.* **1984**, *102*, 146. (b) Sugimoto, T.; Itoh, H.; Mochida, T. *J. Colloid Interface Sci.* **1998**, *205*, 42. (c) Lu, Y.; Yin, Y.; Xia, Y. *Adv. Mater.* **2001**, *13*, 415.

(14) Peanut-shaped colloids formed through phase separation: (a) Skjeltorp, A. T.; Ugelstad, J.; Ellingsen, T. *J. Colloid Interface Sci.* **1996**, *113*, 577. (b) Sheu, H. R.; El-Aasser, M. S.; Vanderhoff Polym. *Mater. Sci. Engl.* **1988**, *59*, 1185. (c) Okubo, M.; Yamashita, T.; Suzuki, T.; Shimizu *Colloid Polym. Sci.* **1997**, *275*, 288.

(15) Random aggregates of colloidal particles: Stöber, W.; Berner, A.; Blaschke, R. *J. Colloid Interface Sci.* **1969**, *29*, 710.

Here we describe an approach that combines templating and attractive capillary forces to self-assemble monodispersed, spherical colloids into complex aggregates with well-controlled sizes, shapes, and internal structures.<sup>16</sup> We now refer to this procedure as TASA, for *template-assisted self-assembly*. We note that templating has been explored by a number of groups as a powerful means to direct and control assembly processes. For example, Velev and Whitesides et al. have exploited the surface confinement provided by liquid droplets to assemble colloidal particles or microfabricated building blocks into spherical objects.<sup>17</sup> Wiltzius, van Blaaderen, Yodh, and Ozin et al. have demonstrated the use of patterned arrays of relieves on solid substrates to grow colloidal crystals having unusual crystalline orientations and/or structures.<sup>18</sup> Whitesides, Aizenberg, and Hammond et al. have explored the potential of patterned monolayers to direct the deposition of colloidal particles onto designated regions on a solid substrate.<sup>19</sup> Although these attempts have fully demonstrated the capability of physical templating in generating assembled structures with specific geometric shapes, their ability to control the size, shape, and/or internal structure of the resultant assemblies still need to be demonstrated or improved. The TASA process described in this article seems to represent the first step toward this goal: a range of well-controlled colloidal aggregates have been generated using this approach.

This article is more than a collection of the results that we have published previously.<sup>16</sup> It also contains a range of interesting observations that we made most recently. For example, in addition to the cylindrical holes that we employed in our previous demonstrations, this paper also discusses the use of templates in other shapes to generate aggregates having more complex structures. A plausible mechanism for this assembly process is also presented based on our in situ observations using an optical microscope. The capillary force was found sufficiently strong to induce a preferential orientation for the assembled aggregates in the plane of the solid substrate. The smallest size of colloidal particles that could be assembled using this procedure has been further extended from  $\sim 1 \mu\text{m}$  down to  $\sim 150 \text{ nm}$ .

## Experimental Section

**Materials and Substrates.** Monodispersed polystyrene (PS) beads (aqueous dispersions) were purchased from Duke Scientific (Palo Alto, CA), Polysciences (Warrington, PA), or Bangs Laboratories (Fishers, IN). Aqueous dispersions of monodispersed silica colloids were obtained from Bangs Laboratories. Mylar films of various thicknesses (20–100  $\mu\text{m}$ ) were purchased from Fralock of Lockwood Industries (Canoga Park, CA). Flat glass substrates (Micro slides No. 2947, Corning Glass Works, Corning, NY) were cleaned by immersion into a stabilized piranha solution (NanoStrip 2X, Cyantek Corporation, Fremont, CA)

(16) (a) Lu, Y.; Yin, Y.; Xia, Y. *Adv. Mater.* **2001**, *13*, 34. (b) Yin, Y.; Lu, Y.; Xia, Y. *J. Am. Chem. Soc.* **2000**, *123*, 771. (c) Yin, Y.; Xia, Y. *Adv. Mater.* **2001**, *13*, 267. (d) Yin, Y.; Lu, Y.; Xia, Y. *J. Mater. Chem.* **2001**, *11*, 987.

(17) (a) Velev, O. D.; Furusawa, K.; Nagayama, K. *Langmuir* **1996**, *12*, 2374. (b) Huck, W. T. S.; Tien, J.; Whitesides, G. M. *J. Am. Chem. Soc.* **1998**, *120*, 8267. (c) Velev, O. D.; Lenhoff, A. M.; Kaler, E. W. *Science* **2000**, *287*, 2240.

(18) (a) van Blaaderen, A.; Ruel, R.; Wiltzius, P. *Nature* **1997**, *385*, 321. (b) Lin, K.-H.; Crocker, J. C.; Prasad, V.; Schofield, A.; Weitz, D. A.; Lubensky, T. C.; Yodh, A. G. *Phys. Rev. Lett.* **2000**, *85*, 1770. (c) Kim, E.; Xia, Y.; Whitesides, G. M. *Adv. Mater.* **1996**, *8*, 245. (d) Yang, S. M.; Ozin, G. A. *Chem. Commun.* **2000**, 2507. (e) Ozin, G. A.; Yang, M. Y. *Adv. Funct. Mater.* **2001**, *11*, 95.

(19) (a) Tien, J.; Terfort, A.; Whitesides, G. M. *Langmuir* **1997**, *13*, 5349. (b) Aizenberg, J.; Braun, P. V.; Wiltzius, P. *Phys. Rev. Lett.* **2000**, *84*, 2997. (c) Chen, K. M.; Jiang, X.; Kimerling, L. C.; Hammond, P. T. *Langmuir* **2000**, *26*, 7825.

and then rinsed with 18 M $\Omega$  water (E-Pure, Barnstead, Dubuque, IA). *Caution: Piranha solution can react violently with organic chemicals and should be handled with extreme care!* These glass slides were finally dried with a stream of filtered nitrogen gas.

**Instrumentation.** The optical micrographs were recorded on a Leica DMLM microscope (bright field, Germany). The scanning electron microscopy (SEM) images were obtained using a field emission microscope (FSEM, JEOL-6300F, Peabody, MA) or an environmental microscope (ESEM, Electroscan 2020, Wilmington, MA). The FSEM was operated with an accelerating voltage of 15 kV. The ESEM was operated with an accelerating voltage of 20 kV and a pressure of  $\sim$ 5 Torr. All samples prepared for SEM studies had been coated with thin layers of gold ( $\sim$ 50 nm in thickness, MRC 822 Sputtersphere, System Control Technology, Livermore, CA) before imaging. The atomic force microscopy (AFM) images were acquired on Nanoscope-III (Digital Instrument, Santa Barbara, CA).

Note that gold coating may cause the spherical colloids to appear "distorted" under SEM, particularly when these beads are in physical contact. Such an artificial distortion could become more significant as the thickness of gold coating increased. In any event, such a distortion has little to do with the TASA process. This argument is also supported by the TEM measurements: the polymer beads only exhibited a very small distortion in shape ( $<$ 1% from the spherical one) under TEM, because no gold coating was involved in the preparation of samples for TEM studies.

#### Formation of Patterned Arrays of Templates on Glass Substrates.

The patterned arrays of templates were fabricated in thin films of photoresist (spin-coated on glass substrates) using conventional, contact-mode photolithography (with rigid chrome masks). In a typical procedure, a uniform thin film of positive photoresist (e.g., AZ-1512, Clariant Corporation, Somerville, NJ) was coated onto the substrate, and soft-baked at 90  $^{\circ}$ C for 30 min. The thickness of this resist was mainly determined by the spin speed, which could be adjusted from 2000 to 5000 rpm. The glass substrate was then mounted for contact proximity printing with a chrome mask containing arrays of the pre-designed patterns. The photoresist was exposed to the UV light on a 3 in. Quintel aligner (Mountain View, CA) and developed under gentle agitation in the AZ-351 developer (Clariant Corporation, 1:4 dilution with 18 M $\Omega$  water). These patterned glass substrates were finally rinsed with 18 M $\Omega$  water and dried in a stream of filtered nitrogen gas.

Negative photoresists and/or multistep exposure were also used in this process to increase the variation of test patterns that can be generated from a limited number of chrome masks. For example, a two-step exposure approach was used to generate the patterned array of rectangular cavities shown in Figure 3C: a thin film of negative resist (NR9-1500P, Futurrex, Franklin, NJ) was exposed to UV light consecutively through two different chrome masks that were patterned with parallel lines of different feature sizes (2  $\mu$ m  $\times$  2  $\mu$ m versus 5  $\mu$ m  $\times$  5  $\mu$ m). The lines on the second photomask were oriented perpendicular to those on the first one. In this case, the lateral dimensions of the rectangular cavities were largely determined by the widths of parallel lines on these two chrome masks.

Anisotropic etching of silicon was carried out in an aqueous solution containing KOH and 2-propanol (2-PrOH) at 65  $^{\circ}$ C (400 mL of H<sub>2</sub>O, 92 g of KOH, and 132 mL of *i*-PrOH) for 10 min.<sup>20</sup> The etching solution was stirred at  $\sim$ 300 rpm. The masks were relief structures of silver (50 nm thick) that were patterned by using a combination of micro-contact printing ( $\mu$ CP) and selective wet etching.<sup>20</sup> Before silicon etching, the native oxide on the silicon wafer was removed by dipping the sample in an aqueous solution of HF/NH<sub>4</sub>F (250 mL of H<sub>2</sub>O, 140 mL of 48% HF, and 65.5 g of NH<sub>4</sub>F) for  $\sim$ 1 min.

**Fabrication of Fluidic Cells.** The key strategy of this TASA process is the dewetting of an aqueous dispersion of spherical colloids that has been confined within a fluidic cell composed of two parallel glass substrates. The surface of the bottom substrate has been patterned with a 2D array of templates (such as cylindrical holes) using photolithography and/or etching. When this dispersion is allowed to dewet slowly across the cell, the capillary force exerted on the rear edge of this liquid

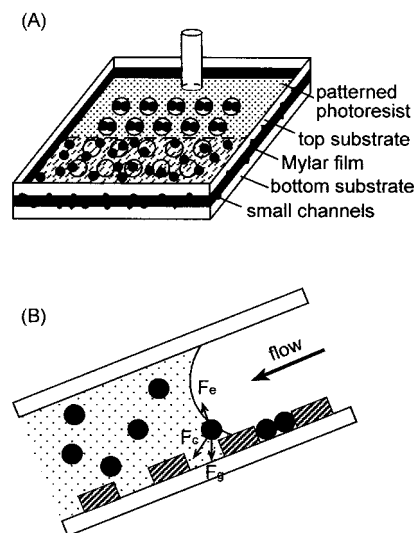


**Figure 1.** (A) A schematic outline of the procedure that was used to assemble colloidal particles into well-defined aggregates. In this case, symmetric dimers were formed in the 2D array of cylindrical holes. (B) A cross-sectional view of the fluidic cell, illustrating the possible forces that may be exerted on the colloidal particles next to the rear edge of the liquid slug: capillary force ( $F_c$ ), gravitational force ( $F_g$ ), and electrostatic force ( $F_e$ ). Depending on the signs of charges on the surfaces of particles and templates, there might exist a repulsive or attractive electrostatic force between their surfaces. Most of the experiments described in the present work involved a weak repulsive interaction, as illustrated in this drawing.

slug will push the spheres across the surface of the bottom substrate until they are physically trapped by the templates. The maximum number of particles that are retained in each template and the structural arrangement among these particles are solely determined by the ratio between the dimensions of the template and the diameter of the spherical colloids.

Figure 1A shows a schematic illustration of the fluidic cell, which was simply constructed by sandwiching a thin frame of Mylar film between two glass substrates.<sup>16</sup> A small hole  $\sim$ 2 mm in diameter was drilled in the top glass substrate, and a glass tube ( $\sim$ 5 mm in diameter) was glued to this hole with epoxy. Before assembly of the cell, the top glass substrate had been rinsed with acetone and 2-propanol, and dried in a stream of filtered nitrogen gas. The glass substrates had been treated with the oxygen plasma of a reactive ion etching (RIE) machine (Phantom RIE, TRION) to make the surface wettable by water. The square frame of Mylar film ( $\sim$ 32  $\mu$ m thick) was cut with scissors and then cleaned with 18 M $\Omega$  water. The cell was often assembled in a clean room, tightened with binder clips, and then brought to the ambient laboratory. The Mylar frame has the dual-function to serve as a spacer between the two glass substrates and as a barrier to control the rate at which the colloidal dispersion will flow through the cell.<sup>21</sup>

#### Assembly of Spherical Colloids into Well-Defined Aggregates.

After the fluidic cell had been assembled, an aqueous dispersion of monodispersed colloids (polystyrene or silica spheres) was injected into this cell through the glass tube. Once the dispersion of colloids had completely filled the void space between the glass substrates, the excess liquid was removed from the glass tube with a syringe. The liquid slug confined between the substrates was then allowed to move slowly (at a rate of  $\sim$ 1 mm/h) due to evaporation and/or flow of the solvent through the channels on the surfaces of Mylar film.<sup>16</sup> The flow rate was found to have no significant influence on the yield of the self-assembled clusters. As shown in Figure 1B, the efficiency of this TASA process seems to be determined by three forces: (i) the capillary force ( $F_c$ ) exerted by the rear edge of the liquid slug; (ii) the gravitational force ( $F_g$ ), which should be less significant for PS because its density ( $\sim$ 1.05 g/cm<sup>3</sup>) matches that of water ( $\sim$ 1.00 g/cm<sup>3</sup>); and (iii) the

(20) Xia, Y.; Kim, E.; Whitesides, G. M. *J. Electrochem. Soc.* **1996**, *143*, 1070.

(21) Lu, Y.; Yin, Y.; Gates, B.; Xia, Y. *Langmuir* **2001**, *13*, 1146.



electrostatic interaction ( $F_e$ ), which is shown as a repulsive force in this illustration. In addition, Brownian motion might also play a significant role for colloids less than  $1 \mu\text{m}$  in diameter.

When the liquid slug dewetted from the bottom surface, the capillary force was sufficiently strong to push the colloidal particles into the template holes, and left almost no colloids on the top surface of the template. If the concentration of colloidal dispersion was high enough, each template would be filled with the maximum number of colloidal particles as determined by geometrical confinement. The colloidal beads within each hole tended to be in physical contact as a result of attractive capillary force caused by solvent evaporation.<sup>22</sup> When a second step of assembly is needed, the cell can be heated at  $\sim 90^\circ\text{C}$  in an oven for about 1 min to fix the positions of colloidal spheres within each template hole. If not fixed, some of the colloidal beads might pop out from the template holes in the subsequent step of assembly, as a result of the Brownian motion.

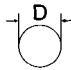


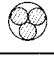
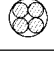
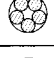
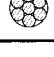
If necessary, the colloidal beads within each template hole can also be fused together into a permanent structure. In this case, the top glass substrate and Mylar frame was removed first, and the bottom glass substrate was placed in an oven and heated at  $\sim 96^\circ\text{C}$  for  $\sim 10$  min. The PS colloids in each aggregate were welded into a single unit due to the viscoelastic deformation of the polymer (probably only at the surface of the polymer bead due to the relatively short time of heating).<sup>23</sup> The photoresist pattern could be removed by dissolving with 2-propanol, and then the bottom substrate could be sonicated in a deionized water bath to release the aggregates of spherical colloids.

## Results and Discussion

We have demonstrated the capability and feasibility of this TASA process by fabricating a variety of polygonal and polyhedral aggregates that are difficult or impossible to generate with other approaches. The experiments based on this self-assembly process have always resulted in the quantitative formation of colloidal aggregates characterized with pre-specified sizes, shapes, and internal structures. Because it is relatively easy and straightforward to change the shape and dimensions of the templates by using the conventional micro lithographic techniques, this approach provides a convenient route to complex structures assembled from colloidal particles.

**Control Over the Structures of Self-Assembled Aggregates.** There are a number of ways to control the size, shape, and structure of aggregates self-assembled from spherical colloids. In our previous demonstrations, we have concentrated on templates in the shape of cylindrical hole because we happen to have such photomasks in our laboratory.<sup>16</sup> Table 1 shows some possible aggregates that could be obtained from this simple system. In this case, the number of spherical colloids that can be retained in each template and thereby the structural arrangement among these colloids are controlled by the ratios between the dimensions (diameter  $D$  and depth  $H$ ) of holes and the diameter ( $d$ ) of the spherical colloids. By simply varying these ratios, one could obtain a range of uniform aggregates having well-defined polygonal or polyhedral shapes. The difference in value between any two adjacent entries in Table 1 illustrates the level of control that one can easily accomplish. Figure 2 shows the SEM images of a few examples of polygonal aggregates that were assembled by templating PS beads against 2D arrays of cylindrical holes. The overall yield of the pre-specified aggregates as calculated from the geometric parameters of the template and the PS beads were usually higher than  $\sim 90\%$ . Common defects were aggregates containing fewer polymer beads than expected. This kind of defect could be

**Table 1.** Control Over the Structure of the Aggregates When Cylindrical Holes Are Used as Templates

Geometric shape of the template	Structures of the cluster	D/d
		1.00-2.00
		2.00-2.15
		2.15-2.41
		2.41-2.70
		2.70-3.00
		3.00-3.30

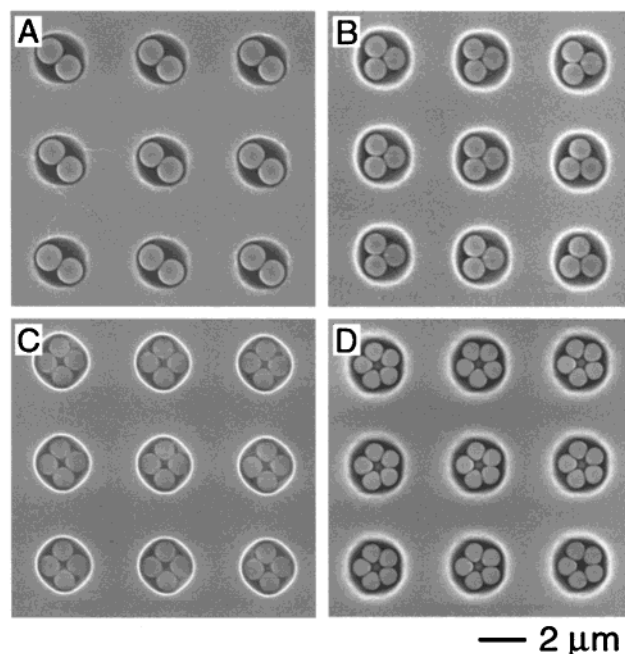


**Figure 2.** The SEM images of some typical examples of polygonal aggregates that were formed by templating PS beads against 2D arrays of cylindrical holes. The cylindrical holes used in all these experiments were  $\sim 2 \mu\text{m}$  in diameter, and the photoresist pattern was still on the substrate. (A) A 2D array of dimers formed from  $1.0 \mu\text{m}$  PS beads; (B) a 2D array of trimers formed from  $0.9 \mu\text{m}$  PS beads; (C) a 2D array of square tetramers formed from  $0.8 \mu\text{m}$  PS beads; and (D) a 2D array of pentagons formed from  $0.7 \mu\text{m}$  PS beads. This TASA approach was able to generate aggregates for all the configurations shown in Table 1. For these polygonal aggregates of PS beads, no significant reduction in the yield was observed when the number of PS beads in each aggregate increased. Note that the spatial orientation of some of the clusters could be changed when the samples were dried through solvent evaporation.

greatly eliminated by varying the concentration of the colloidal dispersion or by flowing a moderately dilute ( $<0.1\%$ ) colloidal dispersion through the fluidic cell more than one time. By optimizing the parameters involved in the TASA process, we have been able to obtain defect-free regions as large as several square millimeters in area that include more than  $\sim 10^5$  elements in the 2D array. At the current stage of development, this number of elements is mainly limited by the areas of test patterns on our photomasks. The self-assembly process, itself, should be extendible to substrates as large as tens of square centimeters in area.

(22) (a) Lazarov, G. S.; Denkov, N. D.; Velev, O. D.; Kralchevsky, P. A.; Nagayama, K. *J. Chem. Soc., Faraday Trans.* **1994**, *90*, 2077. (b) Jackman, R. J.; Duffy, D. C.; Ostuni, E.; Willmore, N. D.; Whitesides, G. M. *Anal. Chem.* **1998**, *70*, 2280.

(23) (a) Mazur, S.; Beckerbauer, R.; Buckholz, J. *Langmuir* **1997**, *13*, 4287. (b) Gates, B.; Park, S. H.; Xia, Y. *Adv. Mater.* **2000**, *12*, 653.

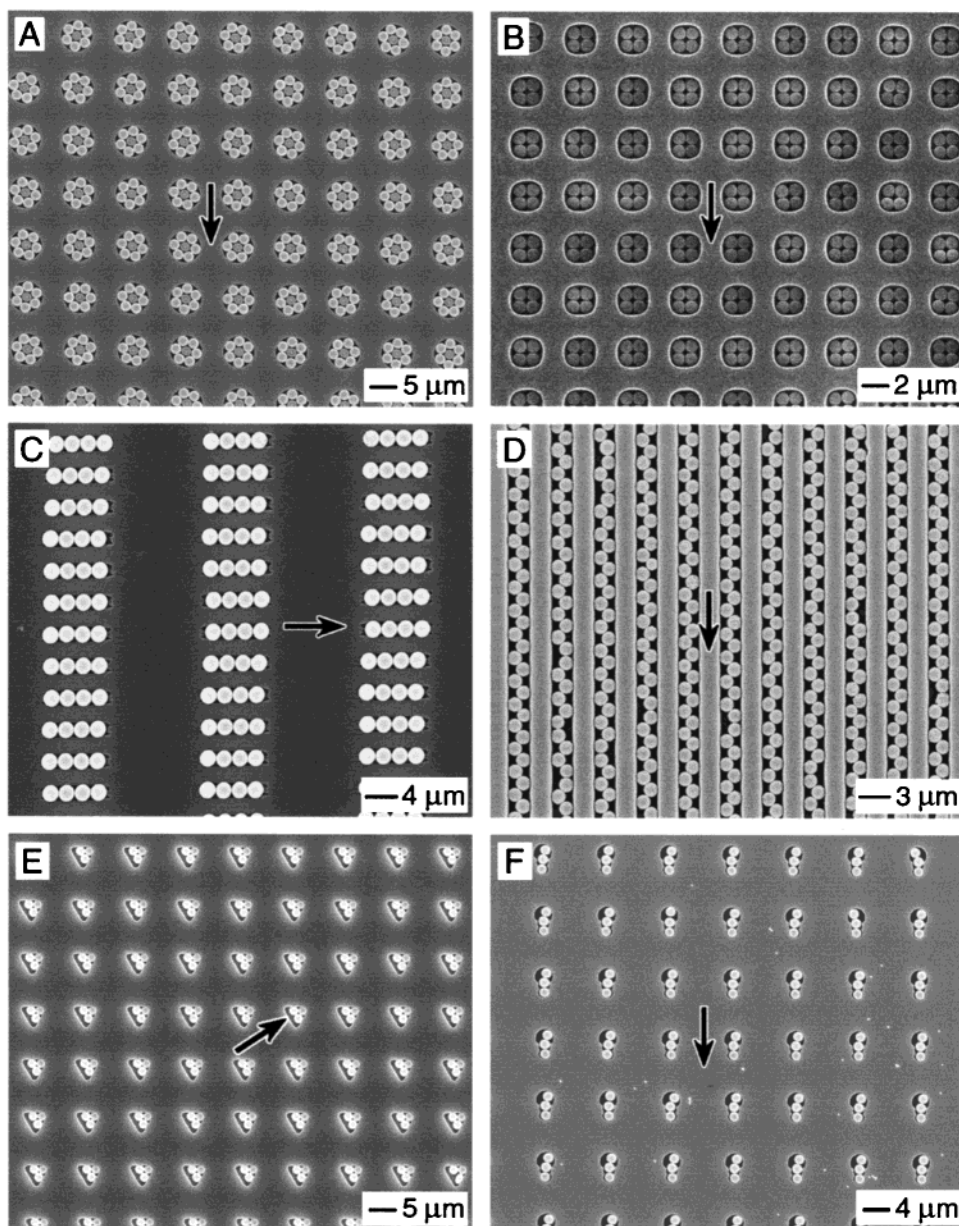


**Figure 3.** The SEM images of 2D arrays of colloidal aggregates that were assembled under the confinement of templates other than cylindrical holes. The arrow indicates the flow direction for the liquid slug. (A) Cylindrical holes ( $6 \mu\text{m}$  in diameter) with  $2\text{-}\mu\text{m}$  posts in their centers, and  $2\text{-}\mu\text{m}$  PS beads; (B) square templates with  $2 \mu\text{m}$  edge length, and  $1\text{-}\mu\text{m}$  PS beads; (C) rectangular templates with lateral dimensions of  $8 \mu\text{m} \times 2 \mu\text{m}$ , and  $2\text{-}\mu\text{m}$  PS beads; (D) trenches  $2.0 \mu\text{m}$  in width and  $2 \text{ cm}$  in length, and  $1.3\text{-}\mu\text{m}$  PS beads; (E) triangular templates with  $5 \mu\text{m}$  edge length, and  $1.75\text{-}\mu\text{m}$  silica spheres; and (F) templates composed of two connected cylindrical holes  $2$  and  $3 \mu\text{m}$  in diameter, and  $1.75\text{-}\mu\text{m}$  silica spheres. Note that the use of noncircular patterns as the templates also allowed one to control the spatial orientation of the colloidal aggregate in the plane of the substrate.

Templates other than cylindrical holes have also been demonstrated to generate aggregates of spherical colloids with other geometric shapes or more complex structures (Table 2). Figure 3A shows the SEM image of an array of six-member rings that were assembled by templating against cylindrical holes with cylindrical posts at their centers. It should also be possible to control the number of polymer beads in each ring by changing its dimensions relative to the polymer beads. Figure 3B shows the SEM image of a 2D array of planer tetramers that were generated by templating against square-shaped holes. The use of a noncircular pattern has also made it possible to control the spatial orientation of the aggregates in the plane of the 2D array. Figure 3C shows the SEM image of a 2D array of linear tetramers that were fabricated by templating against rectangular-shaped holes. Figure 3D displays a parallel 2D array of zigzag chains that were self-assembled by templating against straight

**Table 2.** Control Over the Structure of the Clusters by Using Templates with Other Geometric Shapes

Geometric shape of the template	Structures of the cluster	
		$a = 2d$
		$D = 3d$ $D' = d$
		$L = 4d$ $W = d$
		$d < W < 2d$
		$L = 2.73d$



trenches patterned in a thin film of photoresist. In these two cases, the length of the chain-type aggregates was determined by the longitudinal dimension of the templates, and the internal structure (linear versus zigzag) was defined by the relative ratio between lateral dimension of the templates and the diameter of the spherical colloids. Figure 3E shows the SEM image of a 2D array of triangular aggregates that were assembled by templating against prism-shaped holes. Figure 3F shows the SEM image of a 2D array of bent trimers that were assembled in two interconnected cylindrical holes. Again, it was possible to achieve a preferential orientation (in the plane of the array) for these aggregates by using templates without circular symmetry. These experiments clearly demonstrated that the TASA process described in this paper has the capability to organize spherical colloids into supported 2D arrays of aggregates that have both positional and orientational orders.

**Structural Control Provided by the Vertical Dimension of the Template Holes.** All the examples shown in Figures 2 and 3 are essentially single-layered structures, in which the vertical dimension of the templates is on the same scale as the diameter of the colloidal particles. It was also possible to increase the vertical dimension of the templates in an effort to generate colloidal aggregates with more than one layer (such as polyhedral clusters). Figure 4A shows the SEM image of a sample that was fabricated by templating 1.1- $\mu\text{m}$  PS beads against an array of cylindrical holes that were 2  $\mu\text{m}$  in diameter and height. The dimensions of these cylindrical templates were such that we could only have two PS beads in each template that rested at different levels relative to the bottom of the hole. In this case, an array of tilted dimers (relative to the normal to the substrate) were obtained, with the tilting angles determined by the ratio between the diameter of the cylindrical holes and the diameter of the PS beads. Figure 4B shows the SEM of an array of tetrahedral aggregates that were assembled by templating 1.0- $\mu\text{m}$  PS beads against cylindrical holes that were 2  $\mu\text{m}$  in diameter and depth. By decreasing the size of the PS beads, now we could have two PS beads settled on the bottom of each cylindrical hole, and two additional beads sitting on top of the first layer of PS beads. The tetrahedral structure shown here represented the only arrangement that could survive the strong attractive capillary forces among colloidal particles when the solvent was evaporated. Figure 4C shows the SEM image of another example of two-layered aggregates formed by templating 4.3- $\mu\text{m}$  PS beads against a 2D array of parallel trenches that were 5.0 and 5.5  $\mu\text{m}$  in width and depth, respectively. In this case, the PS beads in the same layer were not in physical contact. Instead, each PS bead in the lower layer was in contact with two beads in the upper level to form a zigzag chain structure along the longitudinal direction of the trench. The inset shows the SEM image of such a chain that had been welded into a concrete piece and subsequently released from the template. We believe the vertical dimension of the templates can be further increased to generate colloidal aggregates with a three-dimensional framework that is much more complex than those illustrated in this paper.

**Formation of Hybrid Aggregates.** We could also greatly increase the complexity of the assembled aggregates by sequentially flowing dispersions of different colloids through the same fluidic cell. The success of this process highly relies on the ability to precisely control the ratio between the dimensions of the template and the diameter of the colloidal particles to ensure that only a well-defined number of particles could be added to the hole in each step. Figure 5A gives the SEM image of a 2D array of 2.8- $\mu\text{m}$  PS beads that were trapped in cylindrical templates ( $D = 5.0 \mu\text{m}$ ,  $H = 2.5 \mu\text{m}$ ) patterned in a thin film of photoresist. The PS bead in each cylindrical

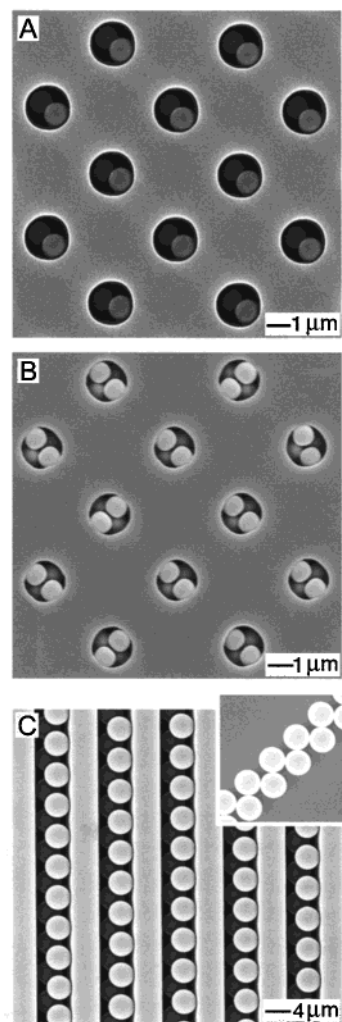


**Figure 4.** The SEM images of 2D arrays of double-layered colloidal aggregates: (A) vertically tilted dimers of 1.1- $\mu\text{m}$  PS beads in cylindrical holes 2  $\mu\text{m}$  in diameter and 2  $\mu\text{m}$  in height; (B) tetrahedrons of 1.0- $\mu\text{m}$  PS beads in cylindrical holes 2  $\mu\text{m}$  in diameter and 2  $\mu\text{m}$  in height; and (C) zigzag chains of 4.3- $\mu\text{m}$  PS beads in trenches that were 5 and 5.5  $\mu\text{m}$  in width and depth, respectively. The inset in part C shows the SEM image of one of these zigzag chains after they had been released from the template and redeposited onto a silicon substrate.

hole was in physical contact with the wall as a result of the shear force (due to the liquid flow) and the attractive capillary force between these surfaces (due to the solvent evaporation).<sup>20</sup> The position of the PS bead in each cylindrical hole could be readily fixed by heating the sample to a temperature slightly higher than the glass transition temperature ( $T_g$ ) of the polymer for about 1 min. This surface that contained a 2D array of polymer beads could then be used in a second step of TASA to add another particle of smaller size into the remaining space of each cylindrical hole. In principle, it should be possible to keep adding colloids with decreasing sizes to a colloidal aggregate to form complex, hierarchical structures. In addition to their difference in size, these colloidal particles could also have different compositions, as well as surface or bulk properties. Figure 5B shows an SEM image of the same sample shown in Figure 5A, after 1.6- $\mu\text{m}$  silica colloids had been added via a second step of TASA. Figure 5C displays the fluorescence microscopy image of a 2D array of asymmetric dimers assembled from PS beads that were not only different in size (3.0 versus 1.7  $\mu\text{m}$  in diameter) but also labeled with different fluorescent organic dyes (FITC and Rhodamin 6G, respectively). In this case, a separate fluorescence image was captured with a

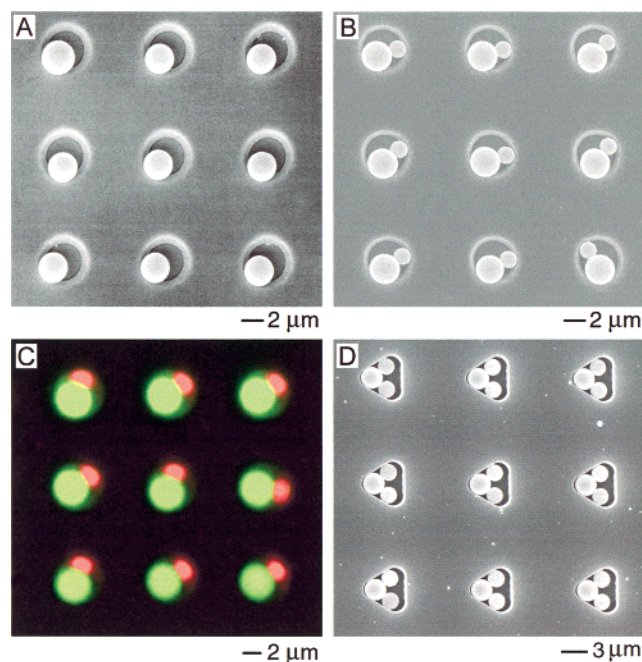


**Figure 5.** (A) The SEM image of a regular 2D array of 2.8- $\mu\text{m}$  PS beads that had been trapped in cylindrical holes 5 and 2.5  $\mu\text{m}$  in diameter and height. (B) An SEM of the same sample after a 1.6- $\mu\text{m}$  silica colloid had been added to each hole through another step of dewetting. (C) The fluorescence microscopy images of an array of asymmetric dimers that were assembled from PS beads that were different in both size and color: 3.0- $\mu\text{m}$  beads doped with a green dye (FITC) and 1.7- $\mu\text{m}$  beads labeled with a red dye (Rhodamine). The green and red dyes were selectively excited, imaged, and then recombined into an overlapped picture. (D) The SEM image of a 2D array of H<sub>2</sub>O-shaped aggregates that were generated using two-step assembly from PS and silica spheres 2.5 and 1.8  $\mu\text{m}$  in diameter, respectively. The edge length of the triangular templates was  $\sim 5 \mu\text{m}$ .

Leica inverted optical microscope (DMIRBE, fitted with blue,  $480 \pm 40 \text{ nm}$ , and green, 515–560 nm, excitation cubes) when the green (or red) dye was selectively excited. The micrograph shown in Figure 5C is a combination of these two images, which indicates a seamless welding between the two beads confined in each template.

The complexity of the self-assembled clusters could also be further increased by using templates having noncircular cross-sections. Figure 5D shows the SEM image of an array of hybrid aggregates that were assembled from 2.5- $\mu\text{m}$  PS beads and 1.8- $\mu\text{m}$  silica colloids. By choosing prism-shaped holes as the template, it has been possible to form H<sub>2</sub>O-shaped aggregates by adding one PS bead and two silica colloids into each template hole through two separate TASA steps. Again, colloidal particles in each hole maintained a close contact due to the attractive capillary force between their surfaces caused by solvent evaporation. Once formed, the particles in each aggregate could be permanently fused into a single piece by heating the sample to a temperature slightly higher than the glass transition temperature of the polymer. These welded aggregates could be subsequently released into a liquid medium by dissolving the photoresist pattern in 2-propanol with sonication. We found that the yield of this multistep TASA process depended on the difference between the diameters of spherical colloids involved in each step. A yield as high as  $\sim 90\%$  has been obtained when the diameters of these colloidal spheres were relatively close to each other (when their difference in size was within 20%).<sup>16b</sup>

**Formation of Free-Standing Aggregates of Spherical Colloids.** Once formed, the internal structure within the colloidal aggregates could be preserved by welding the building blocks

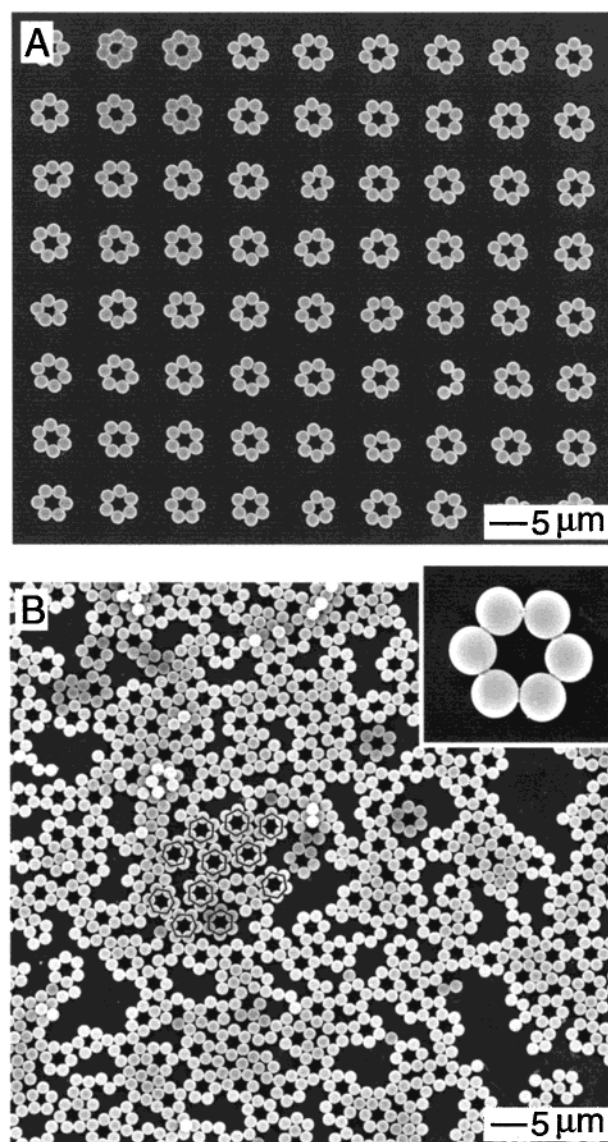


**Figure 6.** (A) The SEM image of an array of ring-shaped aggregates of 2- $\mu\text{m}$  PS beads that were still supported on the original substrate. The photoresist pattern had already been removed by dissolution in ethanol. (B) An SEM image of these aggregates after they had been released from the support and re-deposited onto a silicon substrate. The polymer beads in each aggregate were fused into a single piece by annealing the sample at a temperature slightly higher than the  $T_g$  of the polymer ( $\sim 93 \text{ }^\circ\text{C}$  for PS). Some of these aggregates have been sketched with hexagons to help view individual rings. The inset shows the blow-up SEM image of such a six-membered ring. The percentage of these six-membered aggregates in part B was  $\sim 75\%$ .

into a stable, permanent, single piece. Two approaches can be used here to achieve this goal. The first one induced an adhesion between the colloidal particles by thermally annealing the as-prepared sample at a temperature slightly higher than the glass transition temperature ( $T_g$ ) of the polymer. In this case, the interface between two adjacent polymer beads (or between a polymer bead and a silica bead) within each assembled cluster could be joined together as a result of the viscoelastic deformation of their surfaces.<sup>23</sup> Figure 6A shows the SEM image of a 2D array of six-membered rings that were similar to those shown in Figure 3A. The photoresist template has been dissolved with 2-propanol; the colloidal aggregates still adhered to the surface of the glass substrate as a result of thermal treatment. These fixed aggregates of PS beads could be subsequently released from the substrate by using sonication. Figure 6B shows the



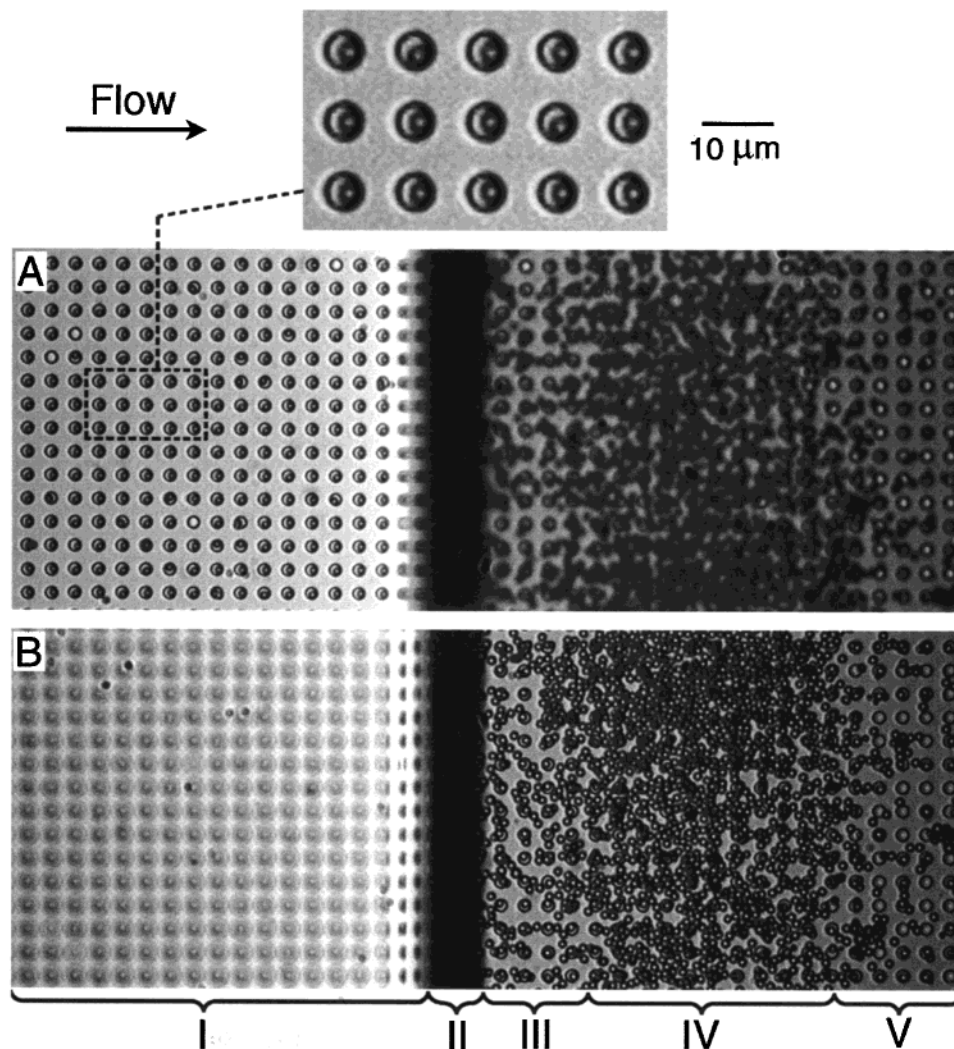


**Figure 7.** Optical microscopy images showing the assembly of 3.1- $\mu\text{m}$  PS beads into 2D array cylindrical holes that were 5 and 2.3  $\mu\text{m}$  in diameter and depth, respectively. The arrow indicates the flow direction. The dark line (region II) in the middle of the image represents the rear edge of the liquid slug. The sample was focused on the (A) dewetted and (B) liquid-filled region of the fluidic cell.

SEM image of these aggregates after they have been released from the original glass substrate and deposited onto a silicon substrate. The inset shows the SEM image of a six-membered ring, indicating the seamless fusion between adjacent PS beads. Although some of these aggregates may have been broken into smaller fragments under the sonication process, the percentage of six-membered rings calculated from this SEM image is still as high as 75%. In a second approach, one could also introduce a relatively strong adhesion between adjacent particles by adding some UV-curable prepolymers into the colloidal dispersion.<sup>24</sup> Some prepolymer liquid could be selectively trapped at the boundary between adjacent colloidal particles, and subsequently served as a glue to hold together all the colloidal particles within each aggregate. It was also helpful to add a sacrificial layer (such as a sputtered film of aluminum or gold) to the glass substrate before photoresist film was spin-coated and patterned. In this case, it was much easier to release the fused aggregates of colloidal particles from the template surface.

**Mechanism of the TASA Process.** As illustrated in Figure 1, the success of this assembly process relies on the balanced interplay between a number of forces. The capillary force created by the meniscus of the liquid rear edge seems to play a crucial role in determining the efficiency of this process. This force has to be strong enough to push colloidal particles into the

template holes and to clean up the top surface of the template when the colloidal dispersion flows across the fluidic cell. As a result, one will only have colloidal particles trapped in the template holes, not on the raised regions of the substrate. Judged from the SEM images that we have taken from dried samples, this capillary force seems to be strong enough to induce a preferential orientation for the colloidal aggregates in the plane of the substrate. This hypothesis was further confirmed by looking at the assembly process in situ through an optical microscope.

Figure 7 shows the optical micrographs that were grabbed during the in situ observation of the assembly process. In this case, the diameter of the PS beads and the cylindrical holes was 3.1 and 5  $\mu\text{m}$ , respectively. Only one polymer bead could be retained in each hole. The direction of liquid flow is indicated by an arrow. The flow of liquid in the fluidic cell was kept perpendicular to the gravitational field in an effort to reduce the influence of gravitational force. The dark line (region II) in the middle of the image represented the rear edge of the liquid slug. Regions III–V (to the right of the dark line) were the portion of fluidic cell that was completely filled with liquid, and region I (to the left of the dark line) represented the empty portion where only the holes were occupied by colloidal particles and water. Because of a large difference in the refractive index between water and air, it was impossible to simultaneously focus

(24) Terfort, A.; Bowden, N.; Whitesides, G. M. *Nature* **1997**, *386*, 162.



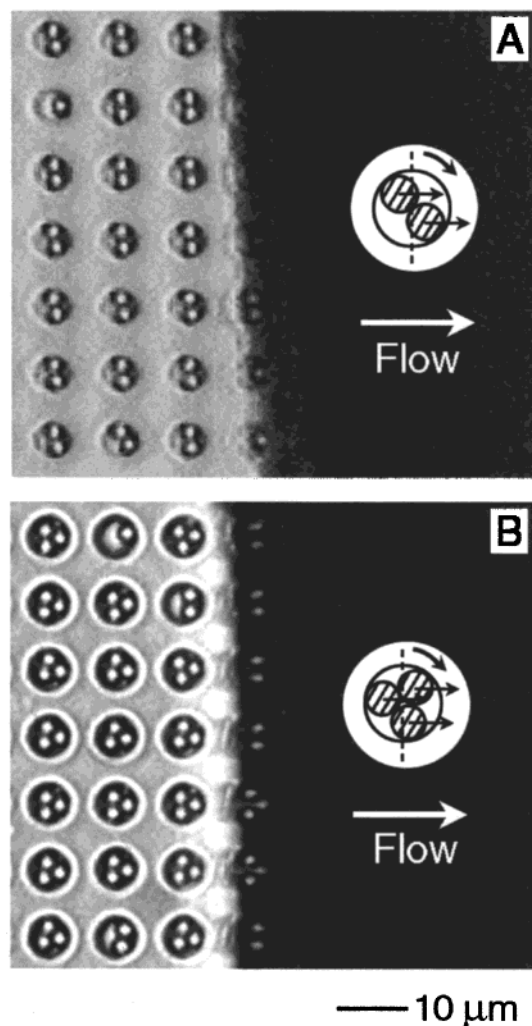


**Figure 8.** Optical microscopy images showing the assembly of 2.5- $\mu\text{m}$  PS beads into (A) dimers and (B) trimers, with cylindrical holes (5 and 6  $\mu\text{m}$  in diameter, respectively, and a depth of 2.3  $\mu\text{m}$ ) as the templates. The dewetted regions were in focus for both images. The direction of flow was indicated by the arrow. Note the preferential orientation in the plane of the template for the self-assembled aggregates. The drawings illustrate how other configurations were rotated to the most stable ones under the action of capillary force and shear force.

on both sides of the cell across the dark line. Figure 7A gives the image where region I was in focus. It can be clearly seen that almost every hole had a sphere physically trapped within it while the top surface of the template was essentially free of particles. This observation indicates that all the particles not trapped by the template holes were dragged along with the liquid by the capillary force exerted on the rear edge of the liquid slug. Another interesting feature is that almost all the PS beads trapped in the holes had been positioned at equivalent sites to yield a regular 2D array of PS beads. Since there was still water in each hole, we believe this spatial ordering was largely driven by the capillary force (along the direction indicated by the arrow) caused by the meniscus of the liquid edge and the shear force induced by the liquid flow. The inset shows the blow-up image of a portion of Figure 7A, from which one can clearly see the preferential positioning of the PS sphere in each hole. Figure 7B shows an optical image of the same sample where the liquid side (regions III–V) was in focus. Because PS beads that were not restrained by the template holes were pushed along with the liquid at a certain speed in the direction indicated by the arrow, they had a maximum concentration in region IV (rather

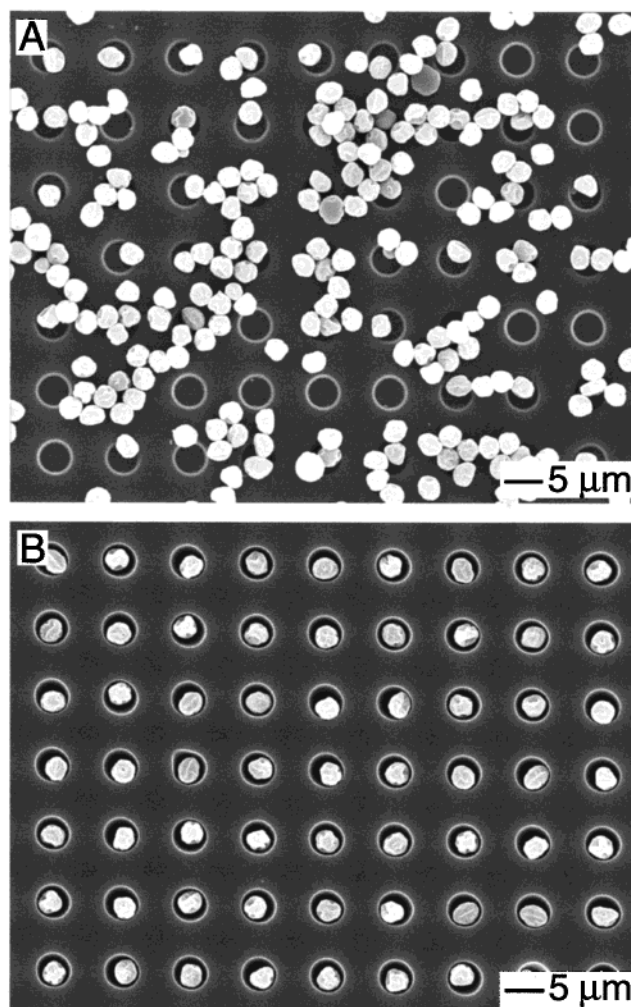


**Figure 9.** The SEM images of two samples that were obtained through the TASA process from PS beads terminated in the  $-\text{NH}_2$  functional group. The pH value of the colloidal dispersion was (A) 6.5 and (B) 8.5, respectively. The strong attraction between PS colloids and template surface for sample A made it hard to move the particles across the surface using capillary force alone. As a result, it was impossible to control the TASA process to generate aggregates with well-defined sizes and structures. When this attractive interaction was reduced by increasing the pH value of the dispersion medium, one could obtain well-defined assemblies through the TASA process. The irregular shape of these colloidal particles was intrinsic to this commercial sample, not caused by the TASA process.

than region III), with a short distance from the edge of the liquid slug. The density of colloidal particles in region V seemed to be similar to that of the original dispersion. In region III, almost every hole had been occupied by a single PS bead, while only a few template holes in region V were occupied by colloidal particles. Different from region I, the trapped colloidal particles in regions III and V were randomly positioned in their template holes.

This in situ observation provides an intuitive insight regarding the mechanism of the TASA process. The colloidal particles in the liquid slug always have certain possibilities of falling into the template holes (as a result of sedimentation). When their concentration is not sufficiently high, only a small portion of the template holes can be occupied (e.g., in region V of Figure 7B). When their concentration becomes high enough, the majority of the template holes will be completely occupied by colloidal particles (as seen in regions III and IV), even before the rear edge of the liquid slug has passed through these regions.

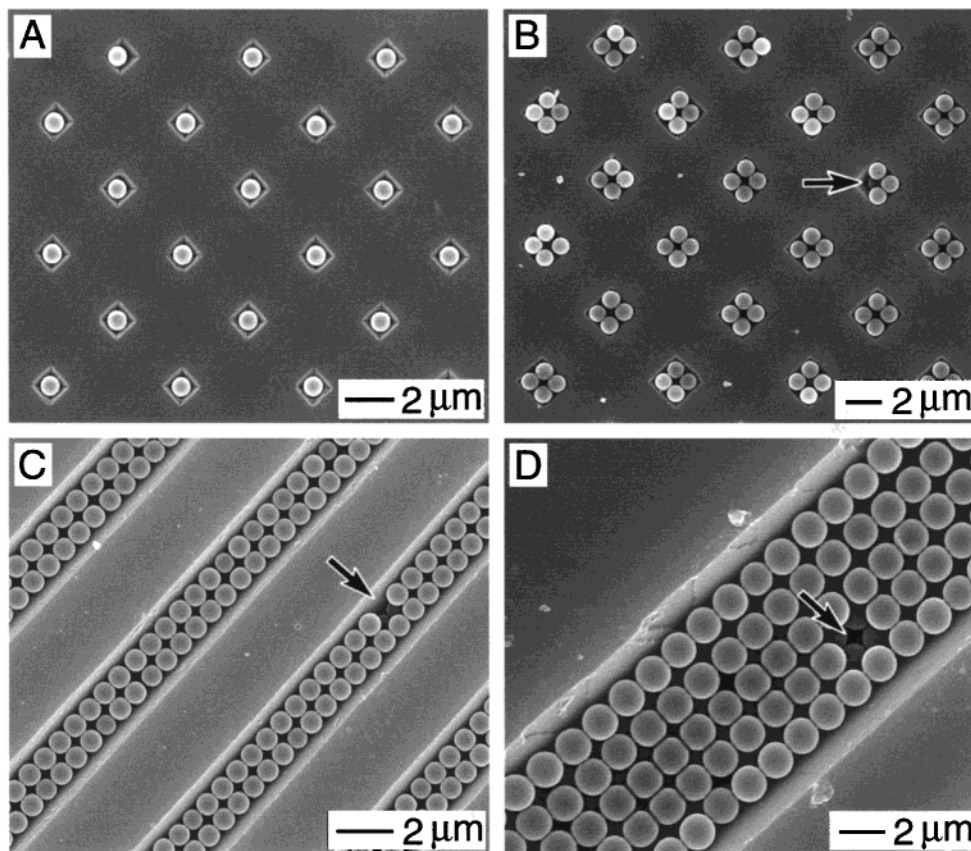


**Figure 10.** The SEM images of 2D arrays of colloidal aggregates that were assembled under the confinement of templates etched in the surfaces of Si(100) substrates: (A) 800-nm PS beads in square pyramidal cavities  $1.2 \mu\text{m}$  wide at the base; (B)  $1.0\text{-}\mu\text{m}$  silica colloids in square pyramidal cavities  $2.2 \mu\text{m}$  wide at the base; (C)  $0.8\text{-}\mu\text{m}$  PS beads in V-shaped grooves  $2.5 \mu\text{m}$  wide at the top; and (D)  $1.6\text{-}\mu\text{m}$  PS beads in V-shaped grooves  $10 \mu\text{m}$  wide at the top. Note that the use of V-shaped grooves as the templates also allowed one to control the orientation of the colloidal crystals. In parts C and D, the face-center-cubic structures have a (100) orientation rather than (111), the one that is most commonly observed when spherical colloids are crystallized into three-dimensional lattices. The arrows indicate defects, where one can also see the colloidal beads underneath the first layer of the structure.

The capillary force has a dual function in this process: serving as a scavenger to clean up the top surface of the template once the liquid has dewetted from it (region I of Figure 7B) and increasing the concentration of colloidal particles in the liquid portion of the fluidic cell (regions III and IV of Figure 7B) by pushing unused particles of region I into these two regions. This hypothesis was further supported by another observation: In most cases, very few template holes in the dewetted region could be filled with colloidal particles when the dewetting process just started. After the edge of the liquid slug had moved forward for a certain distance and enough colloidal particles had been concentrated in regions II–IV, the holes were filled with colloidal particles at a yield approaching 100%. This in situ study also indicates that we can always obtain perfect arrays of colloidal aggregates if the concentration of colloidal particles is high enough. The empty holes that were occasionally observed in the dewetted region I of a template surface could have resulted from local insufficiency of colloidal concentration when the rear edge of the liquid slug moved across the template.

**Control Over the Spatial Orientation of the Colloidal Aggregates.** Because the colloidal particle physically trapped in each template hole is always pushed toward one particular side of the hole in the direction of liquid flow, it seems to be possible to spatially orientate the colloidal aggregates in the plane of the substrate. Figure 8 shows the optical micrographs taken from two separate TASA processes, where two and three PS beads were trapped in each hole, respectively. The arrow indicates the moving direction of the liquid rear edge. Figure 8A clearly indicates that the dimer had been organized such

that its longitudinal axis was perpendicular to the direction of liquid flow. As the rear edge of the liquid passed over the trapped particles, the capillary force (possibly a shear force too) was equally exerted on these two PS beads, dragging them toward the direction of liquid flow. Because these two PS beads experienced a force that is the same in magnitude and direction, there were only two stable configurations for the dimers: either parallel or perpendicular to the flow direction. All other spatial orientations for these dimers were unstable, and should be rotated to one of these two configurations when the liquid edge passed by the hole. The parallel configuration seemed to be less stable relative to the perpendicular one. As shown in the illustration, any small deviation from the perfectly parallel configuration might result in a rotation of the dimer to the perpendicular configuration. This accounts for why the parallel orientation was seldom observed in the assembled aggregates. Figure 8B shows the optical micrograph of an array of triangular trimers that were formed through this TASA process. In this case, the capillary force had again pushed the three PS beads (trapped in each hole) into the most stable configuration with one edge of the triangle perpendicular to the direction of flow. As illustrated in the drawing, other configurations must be rotated to this more stable state when the liquid slug flew across the template holes. There might be another preferential orientation for these trimers (although it was seldom observed in our experiments) where the horizontal PS bead remains to the left of the two vertical PS beads with the triangles orientated as a mirror image to the first configuration. The two demonstrations



described here clearly indicate that the capillary flow is the major force that drives the assembly and spatial ordering of colloidal aggregates.

**Influence of Surface Charges on the TASA Process.** The signs of surface charges on the colloidal particles and the templates were also found to play an important role in determining the efficiency of the TASA process. In principle, there should be a repulsive interaction between the colloidal particles and the surface of the template to ensure that no particle will randomly stick to the templates (including both recessed and raised regions of the substrate). The surface of the as-synthesized silica colloids is often terminated in silanol groups ( $-\text{Si}-\text{OH}$ ) which can ionize to give a negatively charged interface at pH values  $\geq 7$ .<sup>4b</sup> When potassium persulfate is used as the water-soluble initiator, the surface of PS beads prepared through emulsion polymerization is terminated in the negatively charged sulfate group.<sup>4d</sup> Since all the template substrates used in our experiments were treated in oxygen plasma, their surfaces should also be negatively charged at pH values  $\geq 7$ . As a result, there existed a repulsive interaction between the template surfaces and the PS beads or silica colloids used in our TASA process. Because of this repulsive interaction, the colloidal particles could be, somewhat, levitated from the template surface by a certain distance when the colloidal dispersion was flowing through the fluidic cell. Therefore, the capillary force created by the liquid meniscus was able to push the colloidal particles across the surface of the bottom substrate unless they were physically trapped by the template holes.

We confirmed this hypothesis by using colloidal particles whose surfaces were terminated in  $-\text{NH}_2$  groups. In this case, we could switch the sign of interaction between the colloidal particles and template surface by controlling the pH value of the dispersion medium. Figure 9 shows the SEM images of two samples that were prepared from colloidal dispersions with their pH values adjusted to 6.5 and 8.5, respectively. With pH 6.5, there existed an attractive interaction between the positively charged PS beads and the negatively charged template surface ( $-\text{NH}_3^+$ ). The attraction was so strong that it was impossible to push the colloidal particles across the surface and they tended to be randomly deposited on the entire surface of the template in the TASA process. With pH 8.5, this attractive interaction was significantly weakened (or even became slightly repulsive), and we were able to obtain well-defined assembly by templating against the cylindrical holes.

**Influence of the Slope of Template Holes on the TASA Process.** Most of the templates we have evaluated for the TASA process had a  $90^\circ$  slope by which the wall and bottom surface of the template are perpendicular to each other. By varying the exposure and developing times (e.g., overexposure and underexposure), we also generated cylindrical holes in photoresist films that had slopes in the range of  $80$  to  $110^\circ$ . We found that these slight changes in the slope of the template holes had essentially no influence on the efficiency and yield of the TASA process. At the suggestion of a reviewer, we also explored the use of pyramidal cavities and V-grooves etched in Si(100) wafers as the templates for TASA.<sup>20</sup> These types of relief structures have recently been exploited by Ozin et al. in generating on-chip photonic crystals.<sup>18d,e</sup> Figure 10 shows the SEM images of four typical examples. These demonstrations clearly indicate that the TASA process could still be successfully applied to template holes that have a slope as small as  $\sim 54^\circ$ . Note that the procedure described in this paper has also overcome some of the problems associated with the methods previously demonstrated for assembling colloidal beads into well-defined structures. For example, Whitesides et al.<sup>18c</sup> and Ozin et al.<sup>18d,e</sup> placed a flat substrate on the top surface of a

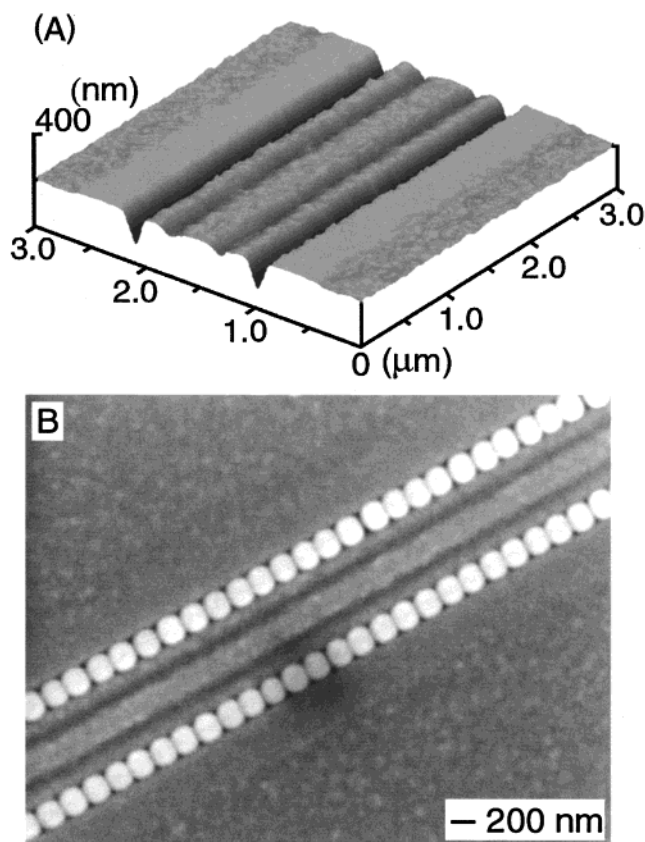


**Figure 11.** (A) An AFM image of the template (a parallel 2D array of trenches that were 150 and 150 nm in width and depth, respectively) that was fabricated using near-field optical lithography. (B) An SEM image of the linear chains that were formed by templating 150-nm PS beads against the trenches shown in part A. These PS beads represent the smallest objects have been successfully incorporated in the TASA process.

template (in direct contact) and then let the colloidal beads assemble into crystalline structures under the confinement of the template. Obviously, this method can only be applied to channel-type templates through which the colloidal dispersion can continuously flow. This method fails when the templates are holes or cavities that are physically separated from each other. Ozin et al.<sup>18c</sup> tried to solve this problem by applying colloidal beads to the template surface through spin-coating. Although this method is simple and convenient to use, the yield of the assembled structures still needs to be improved. The procedure demonstrated in this work solved these problems by placing a spacer (the Mylar film) between the template surface and the top substrate of the cell (Figure 1). As a result, both interconnected and isolated templates could be completely filled with the colloidal beads.

**The Smallest Colloids that Could Be Used in This TASA Process.** At the current stage of development, it is still not clear whether this assembly process can be eventually extended to the nanoscale ( $< 100$  nm). On the basis of what we have observed so far, the answer to this question seems to depend on a number of parameters that still need to be evaluated and optimized—for example, the densities of the colloidal particles and the solvent, temperature, surface tension of the liquid, viscosity of the liquid, sign and density of charges on the surface of the template holes and the colloids, and rate at which the liquid slug moves. All of these parameters ultimately determine the balance of forces exerted on the colloidal particles—that is, the gravitational force, Brownian motion, attractive capillary interactions, and hydrodynamic shear forces. Each one of these

forces may play an important role in determining the yield of this assembly process, as well as the smallest colloids that can effectively serve as the building blocks in this process. We have started to address this issue in our research. At the moment, the major limitation is our ability to fabricate small templates with well-controlled dimensions and well-defined shapes. Figure 11 shows a recent demonstration from our group, which has pushed the size of spherical colloids to the scale of  $\sim 150$  nm. In this demonstration, the templates (parallel 2D arrays of trenches that were  $\sim 150$  nm in width and  $\sim 150$  nm in depth) were fabricated by using the near-field optical lithographic method (with an elastomeric stamp as the binary mask).<sup>25</sup> This demonstration indicated that it was still possible to organize polymer beads as small as  $\sim 150$  nm in diameter into linear chains by using the present method. We believe some modifications to the assembly procedure and development of new materials should be useful when smaller colloids are going to be exploited.

### Conclusions

In summary, we have demonstrated that dewetting of colloidal dispersions from contoured surfaces, attractive capillary forces, and geometric templating could be combined to provide an effective approach for assembling monodispersed colloidal particles into complex aggregates. The experiments described in this article have always resulted in the quantitative formation of uniform aggregates of colloidal particles characterized by a broad range of pre-specified sizes, shapes, and structures. The success of this self-assembly approach has been found to depend on a number of parameters such as the meniscus curvature of the rear edge of the liquid slug, signs of surface charges on the colloidal particles and templates, and concentration of the colloidal dispersion. The smallest colloidal particles that we have

been able to assemble into well-defined aggregates using TASA were  $\sim 150$  nm in diameter. This number was mainly restricted by our capability to generate templates with smaller feature sizes. It is still not clear whether this assembly process can be eventually extended to the nanoscale ( $< 100$  nm), and we believe the ultimate limit to the dimensions of colloidal particles might come from an interplay of Brownian motion and capillary forces.

We believe the availability of well-defined aggregates of colloidal particles will provide an opportunity to experimentally probe the optical, hydrodynamic, and aerodynamic properties of nonspherical colloids with well-characterized, complex morphologies. It will also be interesting to study the interactions between these nonspherical particles to achieve a better understanding on this matter. In addition, the ability to generate hybrid colloidal particles should make it possible to design some experiments that cannot be performed using homogeneous particles. Some of the colloidal aggregates described in this article (such as dimers) could also be explored as the building blocks in other processes of self-assembly to generate meso-structured systems of high complexities that will find use in areas such as photonics, electronics, and condensed matter physics. Even for the self-assembly strategy itself, it might be useful and extendable to other systems that involve different types of building blocks such as cells and vesicles.<sup>26</sup>

**Acknowledgment.** This work was supported in part by a Career Award from the National Science Foundation (DMR-9983893), an Alfred P. Sloan Research Fellowship, a Fellowship from the David and Lucile Packard Foundation, and a New Faculty Award from the Dreyfus Foundation. Y.Y and. Y.L. would like to thank the Center for Nanotechnology at UW for Nanotechnology Fellowship Awards. B.G. thanks the Center for Nanotechnology for an IGERT Fellowship Award supported by the NSF (DGE-9987620).

JA011048V

(25) (a) Aizenberg, J.; Rogers, J. A.; Paul, K. E.; Whitesides, G. M. *Appl. Phys. Lett.* **1997**, *71*, 3773. (b) Yin, Y.; Gates, B.; Xia, Y. *Adv. Mater.* **2000**, *12*, 1426. (c) Li, Z.; Yin, Y.; Xia, Y. *Appl. Phys. Lett.* **2001**, *78*, 2431.

(26) Chia, S.; Urano, J.; Tamanoi, F.; Dunn, B.; Zink, J. I. *J. Am. Chem. Soc.* **2000**, *122*, 6488.